Spectral efficiency limits in crosstalk-impaired multi-core fiber links

Downloaded from: https://research.chalmers.se, 2025-06-18 04:05 UTC

Citation for the original published paper (version of record):

Luis, R., Puttnam, B., Rademacher, G. et al (2018). Spectral efficiency limits in crosstalk-impaired multi-core fiber links. Proceedings of SPIE - The International Society for Optical Engineering, 10551. http://dx.doi.org/10.1117/12.2282822

N.B. When citing this work, cite the original published paper.

research.chalmers.se offers the possibility of retrieving research publications produced at Chalmers University of Technology. It covers all kind of research output: articles, dissertations, conference papers, reports etc. since 2004. research.chalmers.se is administrated and maintained by Chalmers Library

(article starts on next page)

Spectral efficiency limits in crosstalk-impaired multicore fiber links

Ruben S. Luís[a], Benjamin J. Puttnam[a], Georg Rademacher[a], Werner Klaus[a], Erik Agrell[b], Yoshinari Awaji[a], and Naoya Wada[a]

[a]Photonic Network System Laboratory, National Institute of Information and Communication Technology, 4-2-1 Nukui-Kitamachi, Koganei, Japan

[b]Dept. of Signals and Systems, Chalmers University of Technology, SE-412 96 Gothenburg, Sweden

ABSTRACT

We revise the latest advances on ultra-high throughput transmission using crosstalk-limited single-mode multicore fibers and compare these with the theoretical spectral efficiency limits of such systems. We relate the crosstalk-imposed spectral efficiency limits with fiber parameters, such as cladding diameter, core pitch, and trench design. Furthermore, we investigate the potential of techniques such as direction interleaving and high-order MIMO to improve the throughput or reach of these systems when using various modulation formats.

Keywords: Multicore Fiber, MCF, Spatial Division Multiplexing, SDM

1. INTRODUCTION

Spatial division multiplexing (SDM) systems have recently been subject to extensive research, due to the prospect of increasing the throughput of optical networks beyond their forecast requirements.[1] These systems have generally been proposed to support one or more types of SDM media, which include few-mode fibers (FMF) and multicore fibers (MCF).[2] In either case, the throughput of an SDM system approaches that of a corresponding standard single-mode fiber (SSMF) system multiplied by the number of spatial channels.[1] This is particularly evident for SDM systems supported by fiber bundles, where a group of SSMFs within a common cable or duct are used as SDM transmission medium. For more space-efficient media, such as FMFs and MCFs, the interaction between light waves propagating in different spatial channels, referred to here as crosstalk, may lead to performance degradation and consequently a decrease in spectral efficiency (SE). In the case of FMF systems, this interaction is so strong as to require digital demultiplexing mechanisms to recover the transmitted signals.[2] In the case of MCF with uncoupled cores, this interaction is relatively small, such that it may be treated as an additional noise component.[3] These fibers may be distinguished as homogeneous or heterogeneous fibers. Homogeneous MCFs are designed specifically to have nearly identical propagation delay on all the cores. This property will be referred here as inter-core skew (ICS). Low ICS allows implementing synchronized spatial super-channels as well as support multidimensional spatial modulation formats or coding and simplified transmission techniques, such as self-homodyne detection.[4] In contrast, heterogeneous MCFs have very high ICS, which reduces significantly the interaction between light waves in different cores. These fibers provide substantially lower crosstalk levels and have been extensively proposed for long distance transmission.[5]

This work focuses on the performance of SDM systems supported by homogeneous uncoupled core MCFs. We adress the behavior of the crosstalk fluctuations in MCFs when transmitting unmodulated lightwaves and modulated signals. In the later case, we further compare the crosstalk behavior when transmitting carrier-less field-modulated signals with that of carrier-supported intensity-modulated signals. Afterwards, we compare the contributions of crosstalk, amplified spontaneous emission (ASE) noise and nonlinear interference noise (NLIN) in a long distance transmission link to the overall system signal-to-noise ratio (SNR). We show that the characteristics of the fiber can be adjusted to balance the contributions of crosstalk and NLIN by managing the effective area of the cores. Also, we address the dependence of the maximum achievable SE on the number of

E-mail: rluis@nict.go.jp, Telephone: +81 42-327-6873

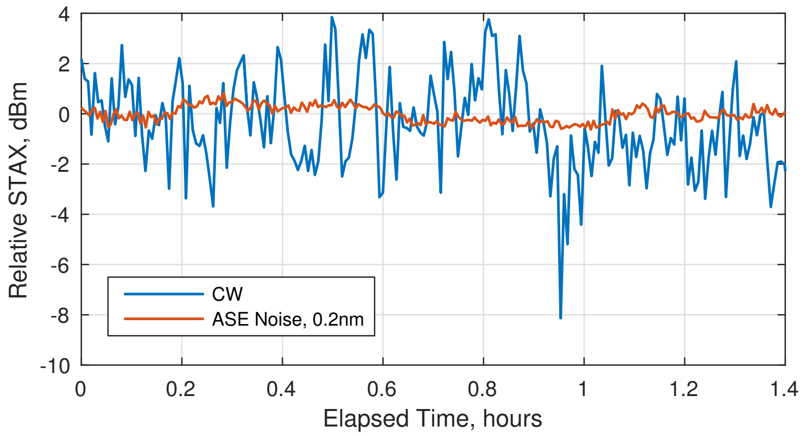

Figure 1. Comparison between the STAX produced between two cores of a 7-core 22 km MCF by a CW signal and filtered ASE noise over a period of 1.4 hours.

cores with optimized effective area. It is shown that although a linear increase of the SE with the number of cores is possible, the SE per core is reduced. Hence improving the performance of these systems requires the use of complex refractive index profiles for each core that improve the confinement of the optical field within the core whilst preserving the remaining fiber parameters. We also address the use of propagation direction interleaving, as a means to reduce the impact of crosstalk in a MCF transmission system without the need to modify the fiber properties. Finally, we revise the latest results in digital compensation of crosstalk with homogeneous MCFs, where joint processing of the signals in multiple cores allows recovering the transmitted signals, effectively eliminating the crosstalk penalty.

2. CROSSTALK IN HOMOGENEOUS UNCOUPLED-CORE MULTICORE FIBERS

Crosstalk in uncoupled core MCFs has been the topic of extensive investigation. In particular, we highlight the works by Hayashi et al.,[3] where its fundamental principles are described. These works have shown that crosstalk in MCFs is distributed along the fiber, which distinguishes it from localized crosstalk in optical components such as couplers or wavelength selective switches. Furthermore, the main contributions of crosstalk along the fiber occur at discrete points, where the waves travelling in different cores are in-phase. These will be referred to here as phase matching points (PMP). The total crosstalk at the output of each core of a MCF results from the sum of the contributions from each PMP, which should be added considering random time-varying phase shifts. As a consequence, the crosstalk in MCFs varies over time, following a chi-square distribution with 4 degrees of freedom.[3] To measure this crosstalk over time, we will define here the average crosstalk, as the long-term average of the crosstalk, and the short-term average crosstalk (STAX), in analogy to copper wire communications systems. The STAX assumes an averaging time window of a few tens of miliseconds, sufficient to obtain a power reading from an optical power meter and can be easily measured. In contrast, the average crosstalk would require a large integration time to be able to capture the full distribution. Fig. 1 shows an example of the variation of the STAX measured in one core of a 7-core MCF over a period of 1.4 hours when illuminating an adjacent core with a constant waveform (CW). The STAX has been normalized to its average. It is shown that the STAX has varied in this fiber during this observation period by as much as 12 dB.

Fig. 1 also shows the variation of the STAX when the interfering core is illuminated with ASE noise with a bandwidth of 0.2 nm. In this case, the crosstalk fluctuations are within less than 1 dB, substantially lower than the CW case. This results from sum of the crosstalk contributions across the ASE noise spectrum, which tends to smooth the overall crosstalk power fluctuations. Ref. 6 has shown that the variance of the STAX depends strongly on the spectral occupation of the crosstalk-generating signals and the ICS. Fig. 2 shows the dependence of the variance of the STAX on the (symbol-rate)$\times$(ICS) product computed using numerical simulation and normalized to the average crosstalk. Also, we considered two different crosstalk-generating signals: a non-return

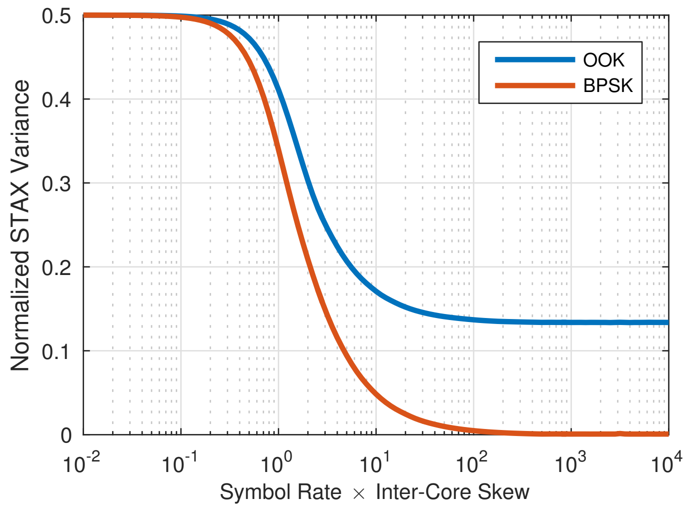

Figure 2. Dependence of the variance of the normalized short term average crosstalk (STAX) on the (symbol-rate)×(ICS) product for a carrier-supported signal (OOK) and a carrierless signal (BPSK). The variance has been normalized to the average crosstalk.

to zero on-off keying (OOK) signal and binary phase-shift keyed (BPSK) signal. With null or low (symbol-rate)×(ICS) product, the system behaves similarly to having a CW as the crosstalk-generating signal, regardless of it's modulation format. When increasing the (symbol-rate)×(ICS) product we find that the STAX variations introduced by opposing frequency components of the crosstalk-generating signal tend to cancel. As a result, for high (symbol-rate)×(ICS) product the STAX fluctuations vanish when using the BPSK signal. Similarly, the STAX variations reduce substantially with the OOK signal but never vanish. This results from the crosstalk contribution introduced by the non-zero OOK carrier. The latter observation is particularly relevant for the application of MCF transmission on short-distance links supporting intra or inter datacenter networks. In contrast, the use of carrier-less field modulation formats such as BPSK, QPSK or higher order QAM over long distance transmission links is most likely to lead to nearly static crosstalk in MCFs. In these conditions, MCF-induced crosstalk may be treated as a nearly Gaussian noise with constant power. This latter case will be the focus of the remainder of this paper.

3. PERFORMANCE OF CROSSTALK LIMITED MULTICORE FIBER SYSTEMS

In this section, we will focus on the case of long distance transmission links using optical field modulation formats supported by coherent detection. Assuming that MCF crosstalk in such systems can be considered Gaussian, we can approximate the SNR at the receiver of the i-th core by:

$$\mathrm{SNR}_i = \frac{P_{\mathrm{s},i}}{P_{\mathrm{ase},i} + P_{\mathrm{nlin},i} + P_{\mathrm{xt},i}} \tag{1}$$

where $P_{\mathrm{s},i}$, $P_{\mathrm{ase},i}$, $P_{\mathrm{nlin},i}$, and $P_{\mathrm{xt},i}$ are the average signal power, ASE noise power, NLIN power and crosstalk power at the output of the i-th core, respectively. The crosstalk power term is given by the sum of the crosstalk contributions of all the interfering cores as:

$$P_{\mathrm{xt},i} = \sum_{j \neq i} X_{j,i}\, P_{\mathrm{s},j} \tag{2}$$

with $X_{j,i}$ as the average crosstalk from core j into core i and $P_{\mathrm{s},j}$ as the power at the j-th core output. We can also rewrite eq. (1) in a form that highlights the contributions of the three noise components to the SNR as:

$$\mathrm{SNR}_i = \left(\mathrm{SNR}_{\mathrm{ase},i}^{-1} + \mathrm{SNR}_{\mathrm{nlin},i}^{-1} + \mathrm{SNR}_{\mathrm{xt},i}^{-1}\right)^{-1} \tag{3}$$

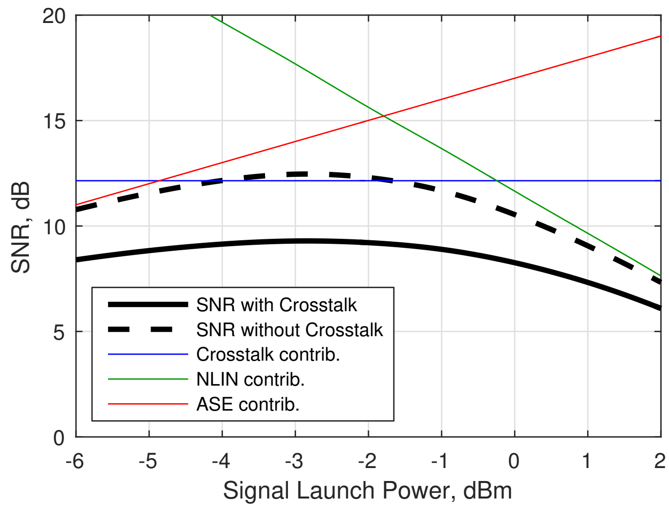

Figure 3. SNR dependence on the signal launch power for the center core of a 40-span MCF link and the corresponding contributions from ASE noise, NLIN and crosstalk.

with $\mathrm{SNR}_{\mathrm{ase},i} = P_{\mathrm{s},i}/P_{\mathrm{ase},i}$, $\mathrm{SNR}_{\mathrm{nlin},i} = P_{\mathrm{s},i}/P_{\mathrm{nlin},i}$, and $\mathrm{SNR}_{\mathrm{xt},i} = P_{\mathrm{s},i}/P_{\mathrm{xt},i}$. Fig. 3 shows an example of the weight of the three SNR contributions as a function of the launched signal power on a 40 span link. The plot presents only the SNR values for the center core of a 7-core fiber with hexagonal disposition of the outer cores and we assumed identical loss and launch power on all cores. Table 1 lists the relevant link parameters and we used the models provided in Ref. 7 and 8 for estimation of the NLIN and the MCF crosstalk, respectively. As in conventional fiber links, increasing the launch power increases $\mathrm{SNR}_{\mathrm{ase},i}$ whilst decreasing $\mathrm{SNR}_{\mathrm{nlin},i}$ due to fiber nonlinearity. In contrast the crosstalk contribution is independent of the launch power.

To improve the SNR of the system, it is possible to modify the fiber design parameters in order to enhance the confinement of the light waves within each core.[9,10] However, in order to maintain the dimensions of the cladding, this must be done at the expense of other fiber characteristics, such as fiber dispersion, attenuation and nonlinearities. A simple method to improve the crosstalk characteristics of a MCF is to reduce the radius of each core.[9,10] Among others, this has the unwanted effects of decreasing the effective area of each core and increasing the cut-off wavelength. In the latter case, we can also need to modify the refractive index delta between the cladding and cores, in order to maintain single-mode operation within the wavelength range of interest. Fig.

Table 1. Computation parameters for the estimation of the SNR of the MCF transmission system shown in Fig. 3.

Parameter	Value	
Multicore Fiber	7	cores
Core Profile	Step Index	
Core Radius	3.9	µm
Core Pitch	38.3	µm
Index Delta	0.53	%
Bend Radius	105	mm
Dispersion Parameter	16.5	ps/nm/km
Attenuation Coefficient	0.2	dB/km
Span Length	80	km
Number of Spans	40	
Symbol Rate	32	GBaud
Channel Spacing	50	GHz
Number of Channels	9	
Amplifier Noise Figure	5	dB

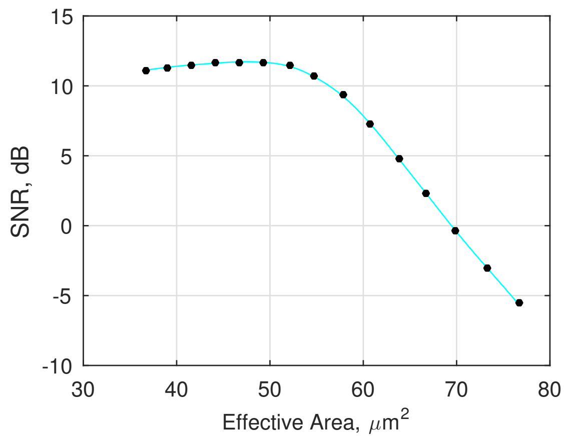

Figure 4. Dependence of SNR of the center core of the fiber described in Table 1 on the effective area of each core. The continuous line is a visual guide.

4 shows the dependence of the maximum achievable SNR of the center core of the fiber described in Table 1 when varying the effective area by changing the core radius and maintaining a cut-off wavelength of 1530 nm, suitable for single-mode operation in the C-band.[9] All remaining fiber properties were assumed constant. It is shown that the SNR may be optimized by balancing the contributions of crosstalk and NLIN for an effective area of 48 μm^2. This is substantially lower than that of a SSMF (aproximately 80 μm^2), which shows that the optimization favored the reduction of crosstalk at the expense of NLIN.

Extending the observations from Fig. 4, we may compute the effective area that optimizes spectral efficiency as a function of the core count, while maintaining the dimensions of the cladding. This is shown in Fig. 5-a) where we varied the number of cores from 5 to 8. As expected, the maximum SE increases nearly linearly with the number of cores. This is achieved by decreasing the effective area and consequently the crosstalk between cores, balancing its contribution with that of NLIN. However, we must note that the increase in SE is substantially smaller than what could be achieved in the absence of crosstalk. This may also be visualized by considering the SE per core, shown in Fig. 5-b). As the number of cores increases the SE per core decreases despite the effort to optimize the effective area. In addition, we must stress that the models used to produce Fig. 4 and Fig. 5 become invalid as the effective area decreases below 35 μm^2 and additional limitations of the fiber must be taken into account, such as attenuation and dispersion. Nevertheless, our approach clearly shows the SE limitations

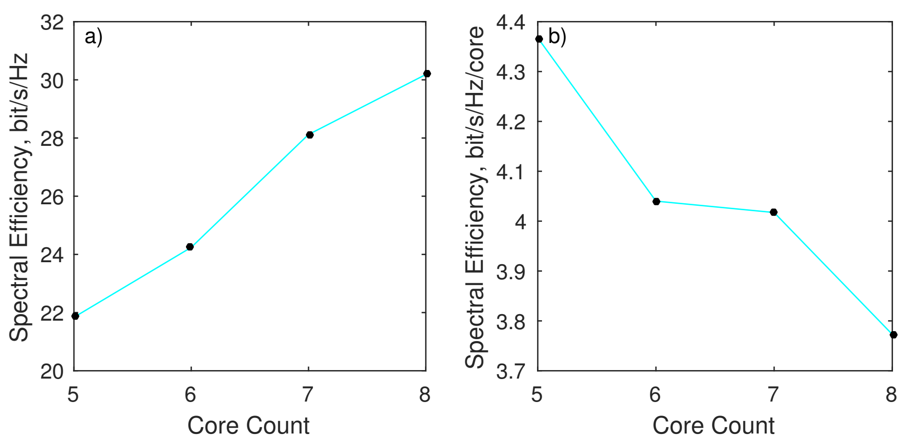

Figure 5. Maximum SE when increasing the number of cores and optimizing the effective area of the fiber described in Table 1.

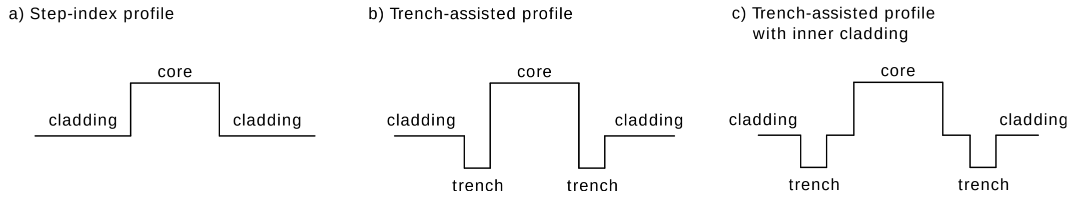

Figure 6. Typical refractive index profiles for core in homogeneous MCFs.

imposed by crosstalk on this system and how the balance between crosstalk and fiber nonlinearities can be used to optimize the SE. To further improve SE, it becomes necessary to depart from the conventional step index cores towards trench assisted cores. In these cases, the field confinement in each core is reinforced using refractive index trenches, allowing substantially less crosstalk whilst maintaining high effective area as well as preserving other characteristics such as waveguide dispersion and bending losses.[9,10]

Examples of trench assisted fiber profiles proposed in the literature are shown in Fig. 6. Fig. 6-a) shows the previously considered step index core profile, which matches the structure used by conventional SSMFs. Fig. 6-b) shows a simple trench structure. The refractive index trench confines the field improving the fiber's crosstalk characteristics without extending substantially the area required for each core. This has been the most commonly used structure for homogeneous MCFs, allowing for a large number of cores in a relatively small cladding area.[10] Finally, Fig. 6-c) shows a more complex core profile where the core is surounded by an inner cladding before the refractive index trench.[11] This structure allowed so far the lowest reported crosstalk levels for an homogeneous MCF whilst preserving the effective area of each core.

Another possible approach to reduce the crosstalk impact in MCF transmission systems is the use of propagation direction interleaving,[12] as illustrated in Fig. 7-a). In these systems, the crosstalk in a given core is minimized by having as many as possible of its neighbors carrying signals in the opposite propagation direction. Ref. 12 has shown that this technique allows reducing the crosstalk by as much as 10 dB for spans of 100 km or less. The residual crosstalk results from backscattering in the fiber as well as reflections occurring in imperfect splices or connectors. This technique requires an optimization of the core positions within the fiber, in order to ensure equal throughput in both directions whilst minimizing the number of neighboring cores with the same propagation direction. Fig. 7-b) shows the core arrangements and propagation directions proposed in Ref. 12 for 12-core MCFs with ring and dual ring core structures, respectively. Optimal core direction interleaving dispositions for different core counts are yet to be reported, to the authors' knowledge.

4. DIGITAL COMPENSATION OF CROSSTALK

In the previous section, we have assumed crosstalk in MCFs as a transmission impairment. However, similarly to what has been performed in FMF transmission systems, the impact of crosstalk in homogeneous MCFs may

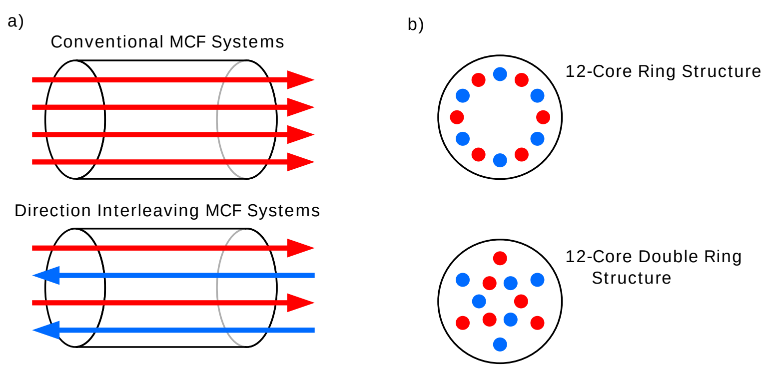

Figure 7. Propagation direction interleaving in MCF transmission systems (a). Core propagation directions for a 12-core fiber with ring structure and double ring structure (b).

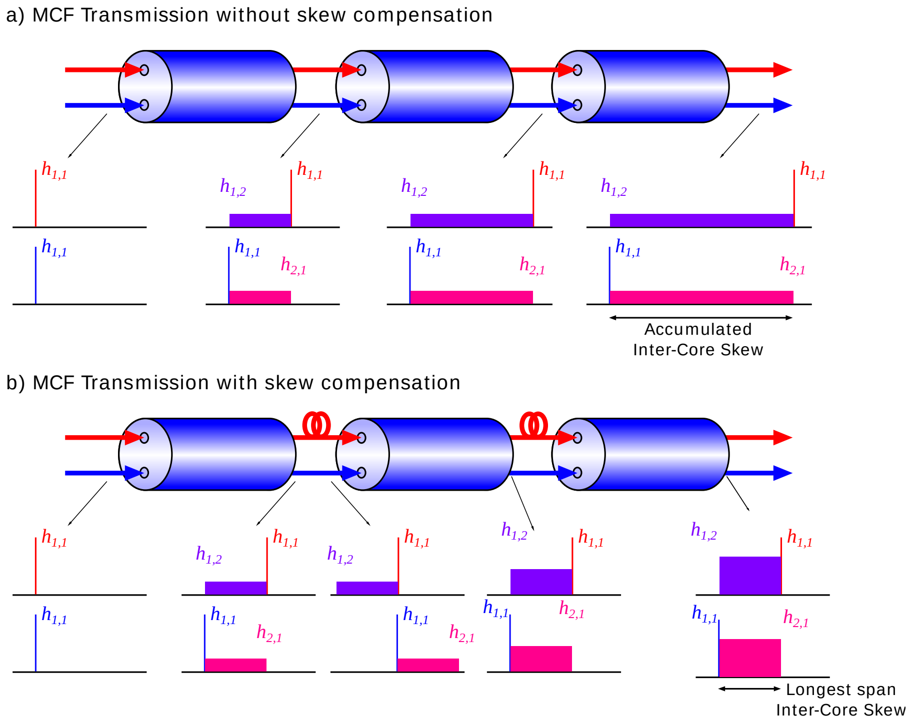

Figure 8. Simplified evolution of a 2-core MCF transmission system's impulse response (a) without ICS compensation and (b) with ICS compensation.

be digitally compensated.[13] The compensation can be performed by jointly processing the received signals from multiple or all cores using typical methods for the inversion of the channel, such as multiple input-multiple output structures. This effectively demultiplexes the jointly processed signals, substantially reducing the crosstalk impact.[13] Similarly to FMF systems, the main limitation to the use of digital demultiplexing mechanisms is the required memory length to encompass the channel impulse response. In the case of FMF systems, this memory typically grows with the square root of the transmission distance due to the strong coupling between spatial channels.[2] In heterogeneous MCFs, the intentionally large ICS leads to long channel memory, which grows linearly with the transmission distance and may potentially be difficult to compensate. Homogeneous MCFs, with intentionally low (but non-negligible) ICS have the potential to support digital demultiplexing schemes due to relatively short channel memory. To address the growth of this memory with transmission distance, Fig. 8-a) illustrates the evolution of the system impulse response along a multi-span 2-core MCF transmission system. For the sake of this example, we assume single polarization signals, absence of fiber nonlinearities, dispersion or attenuation and polarization maintaining fiber. As such, we can define the MCF transfer matrix as having four coefficients, $h_{i,j}$ with i and j referring to the core 1 or 2. In back-to-back, the impulse responses relating the signal on each core to itself, $h_{1,1}$ and $h_{2,2}$ are short, time-aligned impulses. As transmission spans are introduced, the impulses become misaligned due to non-negligible residual ICS. The crosstalk impulse responses $h_{1,2}$ and $h_{2,1}$ relate to the coupling of light between cores that occurs along the transmission fiber. As such, those impulse responses after the first span will have nearly rectangular shapes with a temporal duration corresponding to the ICS of that fiber span. This effect is accumulated on the subsequent spans, leading to crosstalk impulse responses with duration corresponding to the accumulated ICS of the entire transmission system. Assuming that in a worst case scenario, all spans have the same ICS, the required equalizer memory to fully recover these signals would grow linearly with the transmission distance.

The accumulation of ICS over long transmission link may be countered in multiple ways. As an example, core scrambling exploits the differences of ICS between different pairs of cores in the same fiber, leading to a less steep accumulation of ICS. However, to prevent the crosstalk impulse response from growing with the link

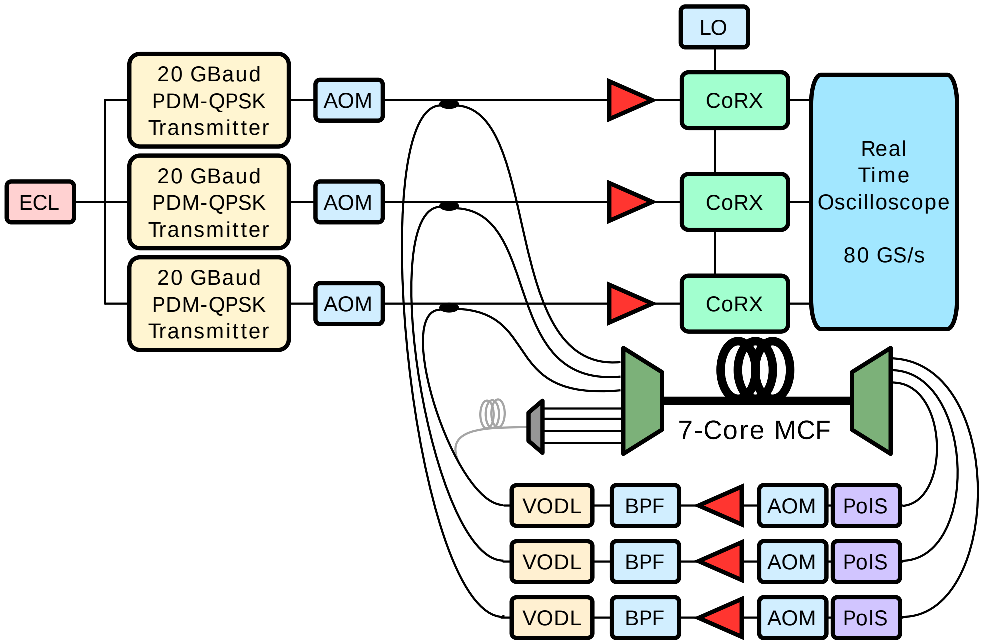

Figure 9. Experimental setup.

length, static ICS alignment mechanisms can be used, as shown in Fig. 8-b). These can be as simple as static delay lines that match the delays of different cores after transmission through each fiber span. When doing so, the crosstalk contributions of each span onto the impulse response superimpose over the same time delay period. As such, the overall crosstalk impulse responses will have a time duration as long as that of the span with the longest ICS. This approach greatly reduces the memory length required to electronically recovery the transmitted signals using MIMO mechanisms. Note that skew compensation mechanisms cannot be supported by FMF systems, where the mixing between spatial modes is very strong, or by heterogeneous MCF systems, where the ICS is potentially too large for practical optical compensation systems.

The ICS compensation technique using static delay lines has been experimentally demonstrated in Ref. 13. There, we have implemented the experimental setup shown in Fig. 9. Three test signals produced by independent 20 GBaud PDM-QPSK transmitters using a shared lightwave where introduced in three synchronized recirculating loops. The loops ran through cores 1, 2 and 3 of a 53.7 km 7-core MCF. The remaining 4 cores of the fiber were illuminated with crosstalk signals produced by extracting and delaying samples of one of the 3 test signals. The outputs of the recirculating loops where detected using three coherent receivers, which shared the same local oscillator light source. The detected signals were synchronously sampled using a 12-channel real-time oscilloscope operating at 80 GS/s. The delays of the 3 test signals at the input of the loop as well as the ICSs of the fiber cores were corrected using variable optical delay lines (VODL). Acousto-optic modulators (AOM), polarization scramblers (PolS) and band-pass filters (BPF) were using for loop switching, compensation of polarization dependent loss and ASE noise filtering, respectively. Erbium doped fiber amplifiers (EDFA) and variable optical attenuators (VOA) where used along the setup to manage optical power. Signal processing was performed offline using C and MATLAB. The DSP was composed of resampling, and normalization stages, followed by a 6×6 MIMO with 2049-tap equalizers. The equalizers were updated using a data-aided least mean squares algorithm. Fig. 10-a) and -b) show the impulse responses of the equalizer taps $h_{p_1,p_2,i,j}$ after transmission through 3222 km and 6444 km, where $p_{1/2}$ refers to the polarization X or Y and i, j refer to the cores 1, 2 or 3. It is shown that the impulse responses corresponding to crosstalk betweem cores are significantly broader than their signal counterparts. We highlighted the taps handling the inter-core crosstalk, which spread over a significant time period as described previously. We noted a crosstalk spread of 40 ns between core 1 and cores 2 and 3, and 15 ns between cores 2 and 3. These values correspond to the ICS of a single span. Comparing Fig. 10-a) with 10-b), where the transmission distance is doubled, one may observe that the duration of the impulse

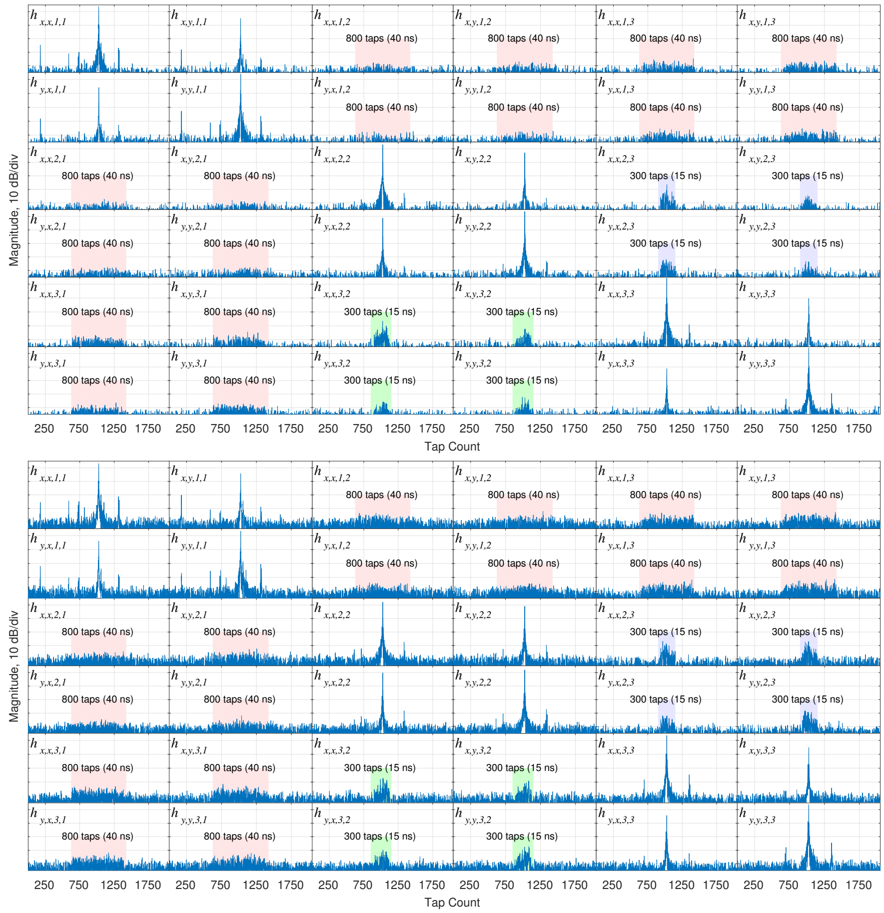

Figure 10. Comparison between the impulse responses of the high order MIMO required to compensate the crosstalk due to MCF transmission after (top) 60 recirculations or 3222 km and (bottom) 120 recirculations or 6444 km.

responses remains the same, supporting the previous claim for the compensation of the ICS.

These results show that the use of electronic demultiplexing mechanisms allows recovering the transmitted signals after transmission through a MCF and consequent crosstalk-induced degradation. However, we stress that this comes at the perhaps excessive cost of very large memory requirements for the recovery mechanisms. This may render this approach unfeasible with current technology unless MCFs with extremely low ICS can be produced.

5. CONCLUSIONS

This paper summarized some of the latest contributions towards ultra-high capacity transmission systems using homogeneous uncouple-core multicore fibers. We have addressed the behavior of crosstalk in these fibers, showing that the variation of the short term average crosstalk tends to fade when the symbol rate or inter-core skew are high. In those conditions, crosstalk may be treated as constant power degradation to the signal-to-noise ratio and we compared its impact with that of amplified spontaneous emission noise and nonlinear interference noise on a long distance transmission link. We've shown that the effective area of each core may be optimized to balance the crosstalk and fiber nonlinearity contributions to the system performance. Finally, we have revised the recent proposal of using joint digital signal processing to demultiplex signals transmitted through a MCF. This technique allows the reconstruction of the original signals after transmission but requires the use of inline inter core skew compensation to reduce the necessary memory length of the digital processing system.

REFERENCES

[1] Richardson, D. J., Fini, J. M., and Nelson, L. E., "Space-division multiplexing in optical fibres," *Nature Photonics* **7**, 354–362 (Apr. 2013).

[2] Shibahara, K., Mizuno, T., Lee, D., and Miyamoto, Y., "Advanced MIMO Signal Processing Techniques Enabling Long-Haul Dense SDM Transmissions," *Journal of Lightwave Technology* (in press) (2017).

[3] Hayashi, T., Sasaki, T., and Sasaoka, E., "Behavior of Inter-Core Crosstalk as a Noise and Its Effect on Q-Factor in Multi-Core Fiber," *IEICE Trans. Commun.* **97**, 936–944 (May 2014).

[4] Puttnam, B. J., Lus, R. S., Agrell, E., Rademacher, G., Sakaguchi, J., Klaus, W., Saridis, G. M., Awaji, Y., and Wada, N., "High Capacity Transmission Systems Using Homogeneous Multi-Core Fibers," *Journal of Lightwave Technology* **35**, 1157–1167 (Mar. 2017).

[5] Mizuno, T., Shibahara, K., Ye, F., Sasaki, Y., Amma, Y., Takenaga, K., Jung, Y., Pulverer, K., Ono, H., Abe, Y., Yamada, M., Saitoh, K., Matsuo, S., Aikawa, K., Bohn, M., Richardson, D. J., Miyamoto, Y., and Morioka, T., "Long-Haul Dense Space-Division Multiplexed Transmission Over Low-Crosstalk Heterogeneous 32-Core Transmission Line Using a Partial Recirculating Loop System," *Journal of Lightwave Technology* **35**, 488–498 (Feb. 2017).

[6] Rademacher, G., Lus, R. S., Puttnam, B. J., Awaji, Y., and Wada, N., "Crosstalk dynamics in multi-core fibers," *Optics Express* **25**, 12020–12028 (May 2017).

[7] Dar, R., Feder, M., Mecozzi, A., and Shtaif, M., "Accumulation of nonlinear interference noise in fiber-optic systems," *Optics Express* **22**, 14199–14211 (June 2014).

[8] Ye, F., Tu, J., Saitoh, K., and Morioka, T., "Simple analytical expression for crosstalk estimation in homogeneous trench-assisted multi-core fibers," *Optics Express* **22**, 23007–23018 (Sept. 2014).

[9] Hayashi, T. and Sasaki, T., "Design strategy of uncoupled multicore fiber enabling high spatial capacity transmission," in [*Photonics Society Summer Topical Meeting Series, 2013 IEEE*], 78–79, IEEE (2013).

[10] Nakanishi, T., Hayashi, T., Shimakawa, O., and Sasaki, T., "Spatial-spectral-efficiency-enhanced multi-core fiber," in [*2015 Optical Fiber Communications Conference and Exhibition (OFC)*], Th3C.3 (Mar. 2015).

[11] Hayashi, T., Taru, T., Shimakawa, O., Sasaki, T., and Sasaoka, E., "Low-crosstalk and low-loss multi-core fiber utilizing fiber bend," in [*Optical Fiber Communication Conference and Exposition (OFC/NFOEC), 2011 and the National Fiber Optic Engineers Conference*], OWJ3 (Mar. 2011).

[12] Sano, A., Takara, H., Kobayashi, T., and Miyamoto, Y., "Crosstalk-Managed High Capacity Long Haul Multicore Fiber Transmission With Propagation-Direction Interleaving," *Journal of Lightwave Technology* **32**, 2771–2779 (Aug. 2014).

[13] Luis, R., Puttnam, B., Rademacher, G., Awaji, Y., and Wada, N., "On the use of high-order mimo for long-distance homogeneous single-mode multicore fiber transmission," in [*European Conference on Optical Communications (ECOC), 2017*], Th.2.F.2 (Sept. 2017).